Distributed Interleaving of Paralleled Power Converters

David J. Perreault, *Member, IEEE*, and John G. Kassakian, *Fellow, IEEE*

Abstract— This paper introduces a distributed approach to interleaving paralleled power converter cells. Unlike conventional methods, the distributed approach requires no centralized control, automatically accommodates varying numbers of converter cells, and is highly tolerant of subsystem failures. A general methodology for achieving distributed interleaving is proposed, along with a specific implementation approach. The design and experimental verification of a 50 kHz prototype system is presented, and quantitative performance comparisons are made between synchronized clocking, independent clocking, and interleaved clocking of the converter cells. The experimental results corroborate the analytical predictions and demonstrate the tremendous benefits of the distributed interleaving approach.

Index Terms— Cellular architecture, distributed conversion, ripple cancellation.

Fig. 1. A cellular converter system supplying a single load.

I. INTRODUCTION

ONE APPROACH to constructing a large power converter system is the use of a cellular architecture, in which many quasi-autonomous converters, called cells, are paralleled to create a single large converter system [1], [2]. As shown in Fig. 1, the cells share the same input and output busses, but are each only required to process a fraction of the total system power. The use of quasi-autonomous cells means that system performance is not compromised by the failure of a cell.

One of the primary benefits of a cellular conversion approach is the large degree of input and output ripple cancellation which can be achieved among cells, leading to reduced ripple in the aggregate input and output waveforms. Consider operation of an N-cell parallel converter system. If all of the cells are clocked synchronously, as illustrated in Fig. 2(a) for a two-cell system, then the system behaves exactly as a single large converter. However, it can be shown that if the cells are clocked independently (and hence operate at slightly different frequencies) as shown in Fig. 2(b), the rms input and output current ripples will be reduced by a factor of $N^{1/2}$ due to the passive (stochastic) ripple cancellation which occurs among cells (Appendix). Active ripple cancellation methods can yield even higher performance benefits. The active method of *interleaving*, illustrated in Fig. 2(c), is well known. (See [3] for a review.) In the interleaving method, the cells are
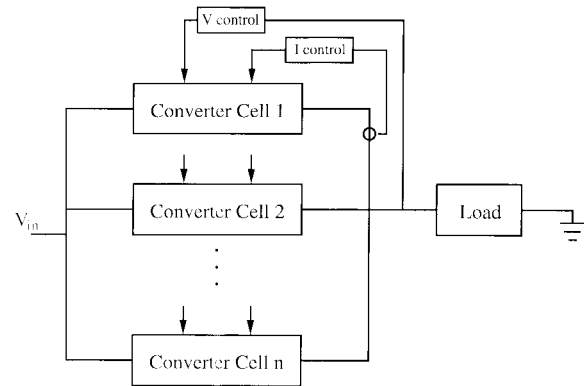
operated at the same switching frequency with their switching waveforms displaced in phase over a switching period. The benefits of this technique are due to harmonic cancellation among the cells, and include low ripple amplitude and high ripple frequency in the aggregate input and output waveforms. For a broad class of topologies, interleaved operation of N cells yields an N-fold increase in fundamental current ripple frequency, and a reduction in peak ripple magnitude by a factor of N or more compared to synchronous operation [3]–[6].

To be effective in a cellular converter architecture, however, an interleaving scheme must be able to accommodate a varying number of cells and maintain operation after some cells have failed. This paper describes a new approach to interleaving parallel (or series) connected power converters. This new approach avoids some of the drawbacks of conventional methods, and is well suited for use in a cellular architecture. A means for implementing the new approach is described, and some of the major design issues are addressed. Experimental results from a three-cell, 50 kHz prototype converter system implementing the approach are also presented, and quantitative performance comparisons are made between synchronized clocking, independent clocking and interleaved clocking of the converter cells.

II. INTERLEAVING

Interleaving N parallel (or series) connected converter cells requires that the cells be operated at the same switching frequency but phase displaced with respect to one another by $2\pi/N$ radians. This is conventionally achieved by using a centralized control circuit to supply properly phased clock or synchronization pulses to the individual cells. Typical
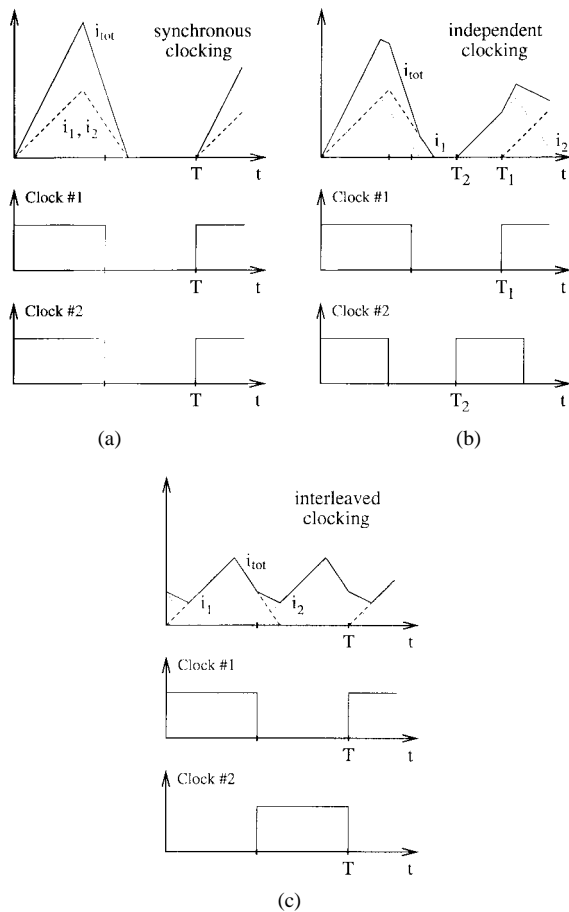
Fig. 2. Clocking and cell current waveforms for paralleled power converters. (a) Synchronous clocking. (b) Independent clocking. (c) Interleaved clocking.

Fig. 3. The distributed interleaving approach.

implementations include the use of a shift register or a counter and decoder to generate the shifted clock pulses [4].

The conventional approach is effective and simple for systems with a fixed number of cells. However, it becomes less practical if there is a varying number of cells in the system, especially if interleaving is to be maintained after failure of one or more cells, as is sometimes desired [2]. The difficulty lies in the circuit and interconnection complexity required to generate the proper number of pulses and direct them to the appropriate cells. Furthermore, any failure of the centralized control circuit will cause failure of the whole system, which is undesirable if high reliability is to be achieved. These limitations have led to the development of the distributed interleaving approach described in this paper.

III. THE DISTRIBUTED INTERLEAVING APPROACH

In the new distributed interleaving approach, the circuitry needed to attain interleaved operation is distributed among the cells, with only minimal connections among cells. The connections among cells are noncritical, i.e., failure of the connection disrupts only the interleaving function, not the basic operation of the system. Unlike the conventional approach, each cell generates its own clock pulses, and only uses intercell information to determine exact frequency and phasing of the local clock. The approach automatically accommodates varying numbers of cells. If an individual cell is removed
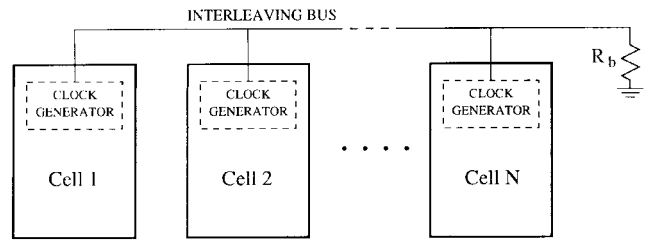
or fails, the remaining cells automatically interleave among themselves. Any failures affecting the information-sharing connections inhibit the interleaving, but do not cause the system to fail. These attributes lead to a flexible, reliable, and robust interleaving system.

To achieve distributed interleaving, all of the cells are connected by an *interleaving bus*, typically consisting of a single wire (Fig. 3). Each cell has its own clock generator, and places information about the frequency and phase of its local clock on the interleaving bus, generally in the form of signals related to the clock waveform itself. Using the aggregated information on the interleaving bus, each cell adjusts the frequency and phase of its own clock to achieve the desired interleaved effect.

IV. A PRACTICAL IMPLEMENTATION METHOD

Consider the implementation of distributed interleaving shown in Fig. 3. Each cell contains its own clock generator. The clock generators are connected together by a single-wire interleaving bus, which is terminated in a known resistance R_b connected to ground. The structure of the clock generator circuit is illustrated in Fig. 4. Each clock generator contains a voltage-controlled oscillator (VCO) whose frequency (and phase) can be varied over a small range with a control voltage. The VCO generates both a sinusoidal and a square wave output voltage. The square wave output is used for the local clock. The sinusoidal output is run through a voltage-to-current converter, which drives a current proportional to the sinusoidal voltage onto the interleaving bus and through R_b. The voltage of the bus will thus be proportional to the vector sum of the sinusoidal VCO outputs of all the cells. Each clock generator senses this voltage and subtracts out its own contribution, leaving a signal which is the aggregate voltage of the other cells. A phase detector compares this signal to the output of the cell's local oscillator. A filtered version of the phase detector output is used for the control input to the VCO. This is done to drive the oscillator 180° out of phase with the aggregate output of the other cells. Each clock generator is thus designed to phase-lock out of phase with the aggregate output of the others.

When the cells are not operating in a locked condition, the voltage on the interleaving bus is the nonzero aggregate of all of the individual clock generator voltages, and the voltage at the input of each cell's phase detector is the aggregate voltage of the other cells. The output of the phase detector is a waveform whose average is either positive or negative depending on whether the aggregate voltage of the other
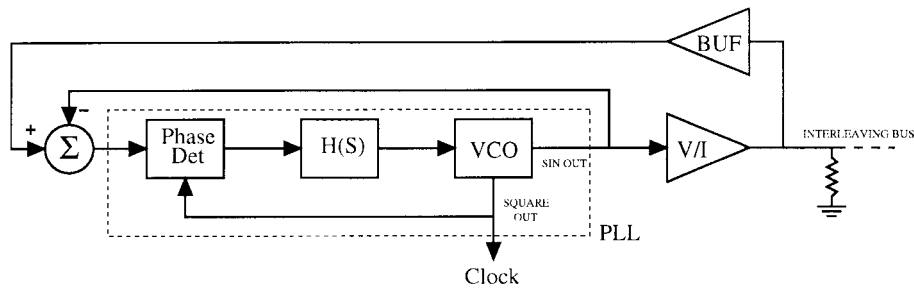
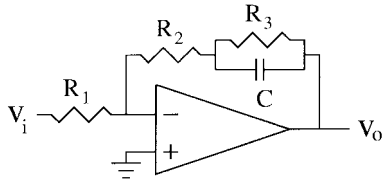Fig. 4.   Structure of the clock generator for the example implementation.

Fig. 5.   Loop filterstructure for the prototype system. $C = 0.22$ μF, $R_1 = 100$ kΩ, $R_2 = 10$ kΩ, $R_3 = 4.3$ MΩ.

Fig. 6.   Input to output phase transfer function for the linearized model of a single prototype clock generator circuit.

cells leads or lags the desired 180° position (relative to the local cell's voltage). When the converter cells are operating in a locked condition, the voltage on the interleaving bus is approximately zero, since the currents injected onto the bus are almost exactly out of phase; the average output voltage of each phase detector only deviates from zero enough to maintain the proper input voltage to its VCO.

When two clock generators are connected to the interleaving bus, they each phase-lock 180° out of phase with the other. When three clock generators are connected, they each phase-lock 180° out of phase with the aggregate of the other two, leading to a locked condition where each clock is 120° out of phase with the others. For situations where more than three clock generators are connected, there is more than one possible locking condition. However, they all involve subgroups of cells interleaving among themselves.

V. SYSTEM DESIGN ISSUES

The design of a distributed interleaving system using phase-locking techniques requires careful attention to the system dynamics. We address the system dynamics in the context of the design of a three-cell prototype system operating at approximately 50 kHz. First, consider the design of the phase-locked loop (PLL) within the clock generator circuit of Fig. 4. The PLL comprises a phase detector, a loop filter $H(s)$, and a VCO [7]. The phase detector generates an output voltage whose average is related to the phase difference between the input waveform and the local oscillator. The multiplier phase detector employed in the prototype system yields a nonlinear relationship which can be modeled as a linear gain ($K_d = 4.8$ V/rad) for small perturbations away from the locked condition. The VCO converts a step in input voltage to a step in output frequency (ramping phase), and hence can be modeled (in a linearized sense) as an integrator with a gain ($K_o = 6289$ rad/(V-s)). The loop filter $H(s)$ serves both to remove high-frequency components from the phase detector output and to compensate the clo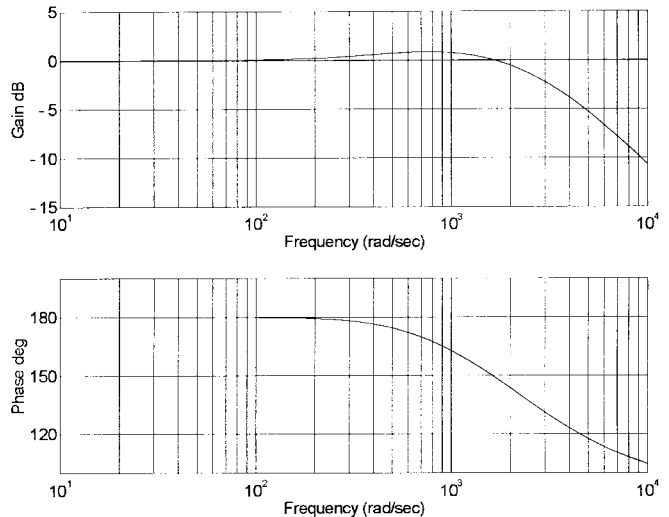sed-loop dynamics of the PLL. To limit the steady-state phase error of the system while allowing a limited degree of play in the phase alignment, an active loop filter of the type in Fig. 5 was selected. As described in [7], this type of loop filter yields a steady-state phase error of

$$\theta_v = \frac{\Delta\omega}{K_o K_d H(0)} \tag{1}$$

where $\Delta\omega$ is the maximum frequency deviation of the oscillator. For the parameters of the prototype system, this yields less than 1.4° of phase error for a 5 kHz frequency deviation, which was deemed acceptable. The resulting PLL design has the (linearized) input to output phase transfer function shown in Fig. 6. This design provided sufficient lock range and tracking range for the task. Note that the 90° phase shift associated with the multiplier phase detector along with an additional 90° phase shift in the VCO sine wave output was employed to achieve the 180° phase lock position desired for the interleaving system. The additional clock generator components are simple op-amp circuits whose dynamics can be neglected in the prototype system.

It must be recognized that the individual clock generators are themselves interconnected in a feedback configuration, yielding closed-loop system dynamics which are a function of the individual clock generator dynamics. We can find the closed-loop dynamics of a two-cell clock generator system using the feedback model of Fig. 7, where we have denoted
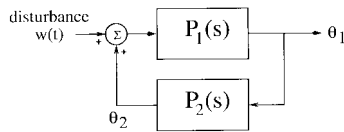
Fig. 7. Feedback model for predicting the dynamics of a two-cell distributed interleaving system.

the (linearized) input to output phase transfer function of the kth clock generator as $P_k(s)$. For the prototype system design, this approach yields closed-loop system poles at $s = -5542$, -496.3, -1.05, and 0 Np/s. The pole at the origin behaves as an integrator, and may at first seem to indicate only marginal stability of the system. However, in reality, this pole merely indicates that a step input phase disturbance can cause the system to settle at a different frequency (e.g., with ramping output phase in the linearized model). Thus, the fact that the desired phase lock condition can occur over a range of frequencies yields the pole at the origin in the linearized model. The limited adjustment range of the VCO's prevents this fact from causing problems. If a disturbance brings one of the clock generators to the edge of its adjustment range, the other clock generator will lock out of phase with it at that frequency with the dynamics of a *single* clock generator. A similar feedback configuration analysis can be made for the three-cell case. This also yields a mixture of stable high- and low- frequency poles and a pole at the origin.

VI. EXPERIMENTAL RESULTS

To validate the proposed implementation, a three-cell low-power boost converter system operating at approximately 50 kHz has been constructed and used to verify the validity of the approach. The converter cells have a boost inductance of 1.5 mH, and operate in discontinuous mode under peak current control. The boost converter system has an output filter capacitance of 0.22 μF, and operates from an input voltage of 15 V. Experimental results presented in this paper are for operation with a load resistance of 390 Ω and a peak cell turn-off current of approximately 55 mA, yielding an output voltage of approximately 25 V.

Each cell employs a conventional UC3843 current-mode control chip with its on-chip oscillator overridden by the local clock generator circuit. The clock generators themselves were constructed with available discrete components: an AD633 differential multiplier was used as a phase detector, while an XR2206 monolithic function generator was used as the VCO. Fig. 8 shows the clock waveforms from the prototype system with two and three converter cells connected to the interleaving bus. Phase locking was found to be very stable with acceptable locking and tracking characteristics for both the two- and three-cell cases. The correct phasing of the clock waveforms to within design specifications (1.5°) is obtained under all conditions. On start up, the clock generators achieve lock within a few seconds, typically settling at the top end of the adjustment range (approximately 57 kHz). This result is consistent with the dynamic model of the previous section. The response speed is far more rapid for small perturbations such as the removal of a cell.
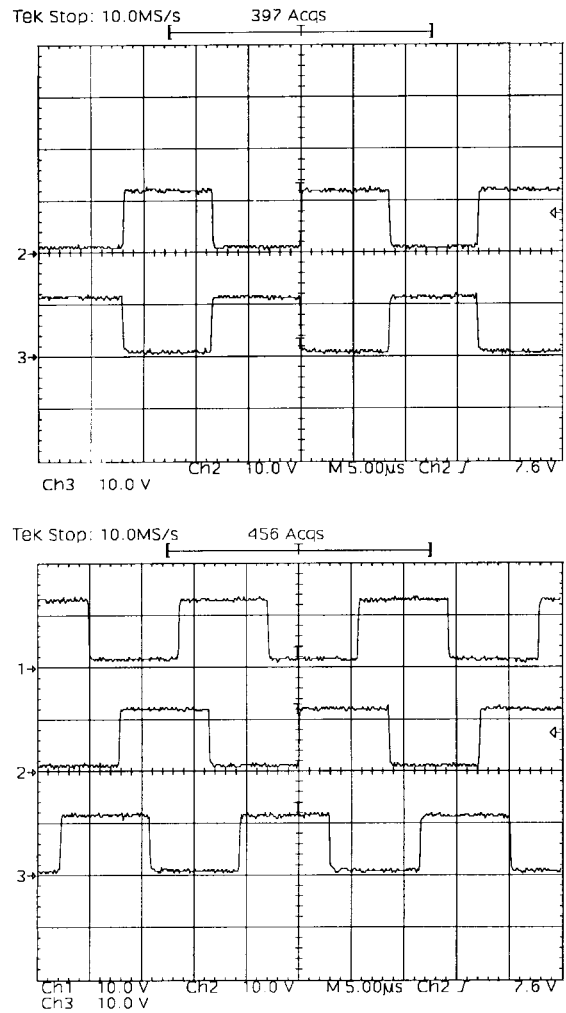

Fig. 8. Experimental clock waveforms for the prototype distributed interleaving system with two and three cells.

To verify the ripple cancellation benefits of the approach, the input current and output voltage ripple were measured with synchronous clocking, independent clocking, and (distributed) interleaved clocking of the three cells. Rms ripple, phase, and frequency measurements were made using the numerical computation functions of a TDS 420 Oscilloscope. As shown in Fig. 9(a), synchronized clocking of the cells leads to an output voltage ripple of approximately 2.1 V_{p-p}, and 0.653 V_{rms}. As shown in Fig. 9(b), independent clocking of the cells (yielding stochastic ripple cancellation) leads to a time-varying output voltage ripple, with the rms ripple reduced down to 0.35 ± 0.03 V_{rms}.

This amount of ripple reduction is consistent with the analysis of the Appendix for independent clocking, and corroborates the results presented there. Operation under distributed interleaving, as shown in Fig. 9(c) and (d), yields a ripple of 0.3 V_{p-p} and 0.072 V_{rms}, with the first major ripple component at three times the individual clocking frequency. This represents a factor of seven reduction in peak-to-peak ripple over synchronized clocking. Ideally, a factor of at least nine reduction should be obtained: a factor of three from the current ripple cancellation, and a factor of three from the frequency increase across the capacitive output filter [3]–[6]. The reason
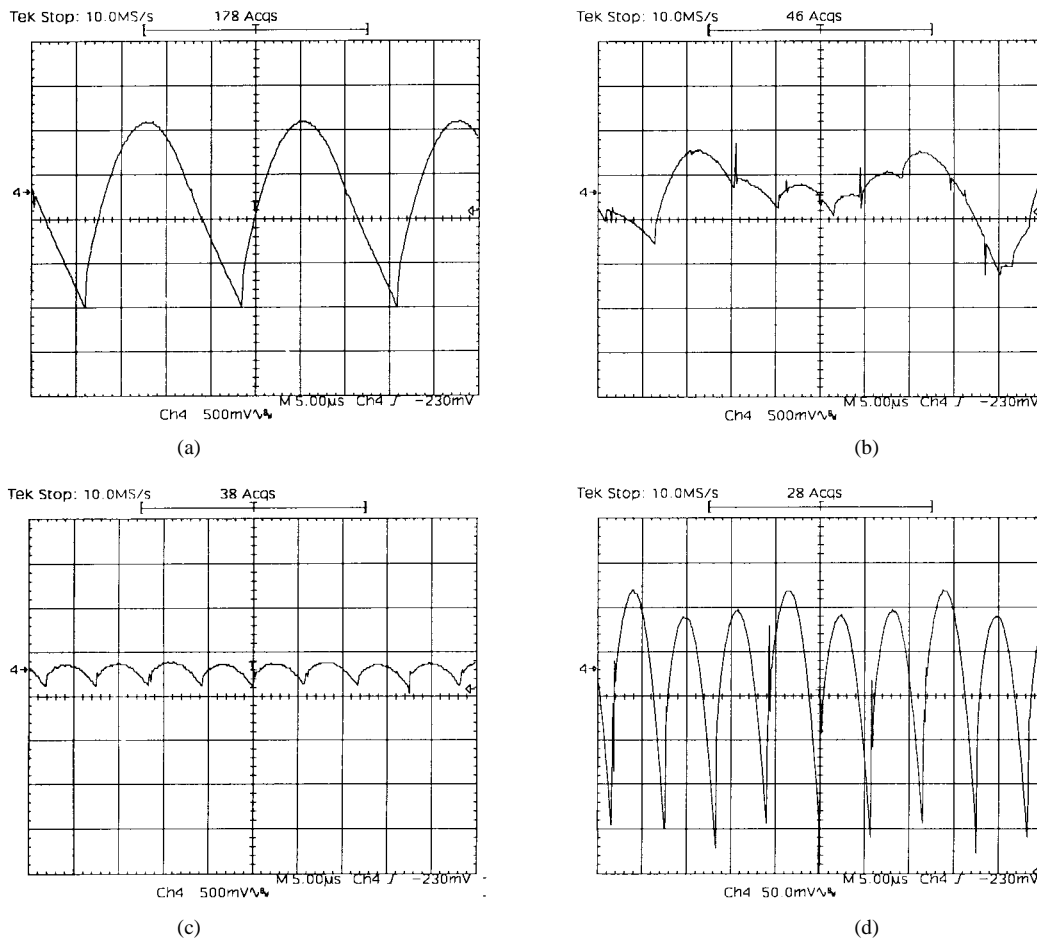
Fig. 9.   Outpuut voltage ripple waveforms for the prototype system. (a) Synchronized clocking. (b) Independent clocking (stochastic ripple cancellation). (c) Interleaved clocking. (d) Interleaved clocking @ 50 mV/div.

for this discrepancy is shown in Fig. 9(d), where it is seen that the cancellation of the fundamental ripple frequency is not perfect due to second order effects such as phasing error, differences in the boost inductors and sense resistors, etc. Nevertheless, use of the prototype distributed interleaving circuitry yields a tremendous performance improvement over both synchronized and independent clocking of the converter system. What may be concluded from these results is that the distributed interleaving approach is practical, and offers large performance benefits without the need for centralized control.

VII. Other Approaches

The distributed interleaving implementation described in this paper generates $2\pi/N$ interleaving for up to 3 cells, above which the locking conditions are as yet unknown. While this may at first seem very restrictive, it should be pointed out that the benefits of interleaving cease to accrue beyond a very limited number of cells due to mismatches among cells [4]. This effect was seen in the prototype system, and is especially true for systems employing distributed current-sharing techniques (where small current mismatches inevitably exist [8]–[13]), and in systems operating at high frequencies (where small time delays correspond to large phase mismatches). For systems with large N, groups of three cells can be interleaved, with

stochastic ripple cancellation occurring among the interleaved groups. Nevertheless, in some cases it may be desirable to generate $2\pi/N$ interleaved clock waveforms for higher numbers of cells. This is achievable through similar means as described here, but at the expense of increased complexity in the clock generator circuit structure and/or the interconnection structure.

VIII. Conclusion

The paper has introduced a distributed approach to interleaving converter cells in which the circuitry required to attain interleaving is distributed among the cells. Unlike conventional methods, the new approach requires no centralized control, automatically accommodates varying numbers of cells, and is highly tolerant of subsystem failures. A general methodology for achieving distributed interleaving has been proposed, along with a specific implementation approach and its experimental verification. Performance of the prototype system under synchronized clocking, independent clocking and interleaved clocking has been measured and compared to analytical predictions. The experimental results corroborate the analytical predictions and demonstrate the tremendous benefits of the distributed interleaving approach.

APPENDIX

This Appendix quantifies the amount of passive, or *stochastic*, ripple cancellation which occurs between paralleled converter cells which are clocked independently. We will show that rms input and output current ripple is reduced by a factor of $N^{1/2}$ with independent clocking as compared to synchronized clocking of the cells. This derivation applies to the case of paralleled converters operating under fixed-frequency PWM control, and is adapted from the approach developed in [14] for paralleled resonant pole inverters.

Consider the output (or input) ripple current i_x due to N identical paralleled converter cells with synchronized clocks. The ripple current is exactly N times the ripple current due to a single cell, and can be expressed as a Fourier series

$$i_x = \sum_{n=-\infty}^{\infty} NC_n e^{jn\omega_0 t} \qquad (2)$$

where

$$\omega_0 = \frac{2\pi}{T}. \qquad (3)$$

The power spectral density of the ripple current is then

$$S_{i_x}(\omega) = 2\pi \sum_{n=-\infty}^{\infty} N^2 |C_n|^2 \delta(\omega - n\omega_0). \qquad (4)$$

This yields an rms ripple current value of

$$i_{x,\mathrm{rms}} = \sqrt{\frac{1}{2\pi} \int_{-\infty}^{+\infty} S_{i_x}(\omega) \, d\omega} = \sqrt{\sum_{n=-\infty}^{\infty} N^2 |C_n|^2}. \qquad (5)$$

Now we consider operation of the converter cells with independent clocking, where the kth cell operates with a clock period $T_k \approx T$. We can express the ripple current of the kth converter cell as

$$i'_{\mathrm{rip},k} = \sum_{n=-\infty}^{\infty} C_{k,n} e^{jn\omega_k t} \qquad (6)$$

where

$$\omega_k = \frac{2\pi}{T_k}. \qquad (7)$$

The shape of the ripple current waveform is independent of the switching period T_k, while the magnitude of the ripple current is proportional to it. The magnitudes of $C_{k,n}$ are therefore proportional to T_k, while the phases of $C_{k,n}$ do not depend on T_k. Thus, as long as the switching periods of the cells are relatively close, we may approximate

$$C_{k,n} \approx C_n. \qquad (8)$$

The percent error in this approximation is equal to the percent difference between T_k and T. The power spectral density of the kth cell's ripple current is

$$S_{i'_{\mathrm{rip}},k}(\omega) = 2\pi \sum_{n=-\infty}^{\infty} |C_{k,n}|^2 \delta(\omega - n\omega_k). \qquad (9)$$

Because the T_k's are not identical due to independent clocking, the power spectral density of the total ripple current

is the sum of the power spectral densities of the individual cell ripple currents. Thus, the power spectral density of the total ripple current i'_x is

$$S_{i'_x}(\omega) = 2\pi \sum_{k=1}^{N} \sum_{n=-\infty}^{\infty} |C_{k,n}|^2 \delta(\omega - n\omega_k)$$

$$\approx 2\pi \sum_{k=1}^{N} \sum_{n=-\infty}^{\infty} |C_n|^2 \delta(\omega - n\omega_k). \qquad (10)$$

This leads to an rms ripple current of

$$i'_{x,\mathrm{rms}} = \sqrt{\frac{1}{2\pi} \int_{-\infty}^{+\infty} S_{i'_x}(\omega) \, d\omega}$$

$$\approx \sqrt{N \sum_{n=-\infty}^{\infty} |C_n|^2} \approx \frac{i_{x,\mathrm{rms}}}{\sqrt{N}}. \qquad (11)$$

Thus, the rms ripple current with independent clocking is a factor of $N^{1/2}$ lower than that obtained with synchronized clocking of the cells. A similar reduction in rms input and output voltage ripples is also to be expected.

REFERENCES

[1] J. G. Kassakian, "High frequency switching and distributed conversion in power electronic systems," in *Proc. Sixth Conf. Power Electron. Motion Contr.*, Budapest, Hungary, 1990, pp. 990–994.
[2] J. G. Kassakian and D. J. Perreault, "An assessment of cellular architectures for large converter systems," in *Proc. Int. Power Electron. Motion Contr. Conf.*, Beijing, PRC, 1994, pp. 70–79.
[3] B. A. Miwa, D. M. Otten, and M. F. Schlecht, "High efficiency power factor correction using interleaving techniques," *IEEE Applied Power Electron. Conf.*, Boston, MA, 1992, pp. 557–568.
[4] B. A. Miwa, "Interleaved conversion techniques for high density power supplies," Ph.D. dissertation, Dept. Elect. Eng. Comput. Sci., Mass. Inst. Technol., June 1992.
[5] C. Chang and M. Knights, "Interleaving technique in distributed power conversion systems," *IEEE Trans. Circuits Syst. I*, vol. 42, pp. 245–251, May 1995.
[6] C. Chang, "Current ripple bounds in interleaved DC-DC power converters," in *Proc. 1995 Int. Conf. Power Electron. Drive Syst.*, Singapore, 1995, vol. 2, pp. 738–743.
[7] F. Gardner, *Phaselock Techniques*. New York: Wiley, 1966.
[8] M. Jordan, "UC3907 load share IC simplifies parallel power supply design," *Unitrode Applicat. Note U-129*, Unitrode Corp., Merrimack, NH.
[9] K. Small, "Single wire current share paralleling of power supplies," U.S. Patent 4 717 833, 1988.
[10] D. J. Perreault, R. L. Selders, and J. G. Kassakian, "Frequency-based current-sharing techniques for paralleled power converters," in *1996 IEEE Power Electron. Special. Conf.*, 1996, pp. 1073–1079.
[11] R. Wu, T. Kohama, Y. Kodera, T. Ninomiya, and F. Ihara, "Load-current-sharing control for parallel operation of DC-to-DC converters," in *Conf. Rec. IEEE Power Electron. Special.*, Seattle, WA, 1993, pp. 101–107.
[12] T. Kohama, T. Ninomiya, M. Shoyama, and F. Ihara, "Dynamic analysis of parallel module converter system with current balance controllers," in *Conf. Rec. 1994 IEEE Telecommun. Energy*, 1994, pp. 190–195.
[13] V. J. Thottuvelil and G. C. Verghese, "Stability analysis of paralleled DC/DC converters with active current sharing," in *IEEE Power Electron. Special. Conf.*, 1996, pp. 1080–1086.
[14] D. J. Perreault and J. G. Kassakian, "Analysis and control of a cellular converter system with stochastic ripple cancellation and minimal

magnetics," *IEEE Trans. Power Electron.*, vol. 12, pp. 145–152, Jan. 1997.

[15] _____, "Distributed interleaving of power converters," in *Proc. Seventh Int. Power Electron. Motion Contr. Conf.*, Budapest, Hungary, Sept. 1996, pp. 2/149–2/153.

David J. Perreault (S'91–M'97) was born in North Providence, RI, on January 22, 1967. He received the B.S. degree from Boston University, Boston, MA, in 1989, and the S.M. and Ph.D. degrees from the Massachusetts Institute of Technology (MIT), Cambridge, in 1991 and 1997, all in electrical engineering.

He is currently a post-Doctoral Researcher with the MIT Laboratory for Electromagnetic and Electronic Systems, where his work includes research and development of cellular power electronic architectures.

Dr. Perreault is a member of Tau Beta Pi, Sigma Xi, and the National Society of Professional Engineers.

John G. Kassakian (S'65–M'73–SM'80–F'89) received the Sc.D degree from the Massachusetts Institute of Technology (MIT), Cambridge, in 1973.

He is a Professor of electrical engineering and Director for the MIT Laboratory for Electromagnetic and Electronic Systems. His fields of expertise are power electronics and automotive electrical systems, and he serves as a consultant to government and industry. He has published extensively in the area of power electronics, and is a coauthor of the textbook *Principles of Power Electronics*.

Dr. Kassakian was the Founding President of the IEEE Power Electronics Society and serves as the U.S. representative to the European Power Electronics Society. He is the recipient of the IEEE Centennial Medal, the IEEE William E. Newell Award, the IEEE Distinguished Lectureship Award, and the Distinguished Service Award. In 1993, he was elected to the National Academy of Engineering.